



Phosphoenolpyruvate carboxylase (PEPC) is essential for the glycolytic pathway and parasite proliferation in *Babesia gibsoni*

Dong-Fang Li^{1,3}, Ling-Na Wang^{1,3}, Yi-Dan Bai^{1,3}, Yu-Xin Yu^{1,3}, Xing Lu^{1,3}, Xing-Ai Guan^{1,3}, Fang-Jie Li^{1,3}, Sen Wang^{1,3}, Lan He^{1,2,3*} and Jun-Long Zhao^{1,2,3*}

Abstract

Apicomplexan parasites predominantly generate ATP and lactic acid through glycolysis and anaerobic glucose metabolism, incorporating CO₂ into glycolysis via a stage-dependent phosphoenolpyruvate carboxylase (PEPC) mechanism. Although the role of PEPC in plant and bacterial carbon fixation is well documented, its function within *Babesia* remains largely unexplored. This study employs reverse genetics to probe the biological role of PEPC in *Babesia gibsoni*, noting its conservation across similar protozoa, suggesting a pivotal and conserved biological function. Western blotting and immunofluorescence (IFA) experiments using the BgPEPC-3 × Flag strain revealed that the BgPEPC protein has a molecular weight of 105 kDa and localizes predominantly to the cytoplasm. Attempts to knock out the PEPC gene in BgPEPC-3 × Flag strains failed under standard media conditions, succeeded only with the addition of 5 mM malate, an upstream metabolite of oxaloacetic acid (OAA). In addition to malate, the downstream metabolite of OAA can also partially compensate for the phenotypic defects caused by PEPC deficiency. This intervention alleviated severe growth deficits, underscoring the critical role of aspartate in the parasite life-cycle. Moreover, metabolic inhibitors such as L-cycloserine and triazamidine, which target aspartate aminotransferase and mitochondrial functions, respectively, demonstrated increased efficacy against BgPEPC knockout strains. The lack of a compensatory response to malic acid supplementation underscores the integral role of BgPEPC in intermediary carbon metabolism and its necessity in providing aspartate as a precursor to pyrimidine synthesis. Collectively, these findings suggest that PEPC could be a potential target for future drug development against *B. gibsoni* infections.

Keywords *Babesia gibsoni*, Phosphoenolpyruvate, Phosphoenolpyruvate carboxylase, Malate, Aspartate

handling editor: Shuai Wang.

*Correspondence:

Lan He

helan@mail.hzau.edu.cn

Jun-Long Zhao

zhaojunlong@mail.hzau.edu.cn

¹National Key Laboratory of Agricultural Microbiology, College of Veterinary Medicine, Huazhong Agricultural University, Wuhan, China

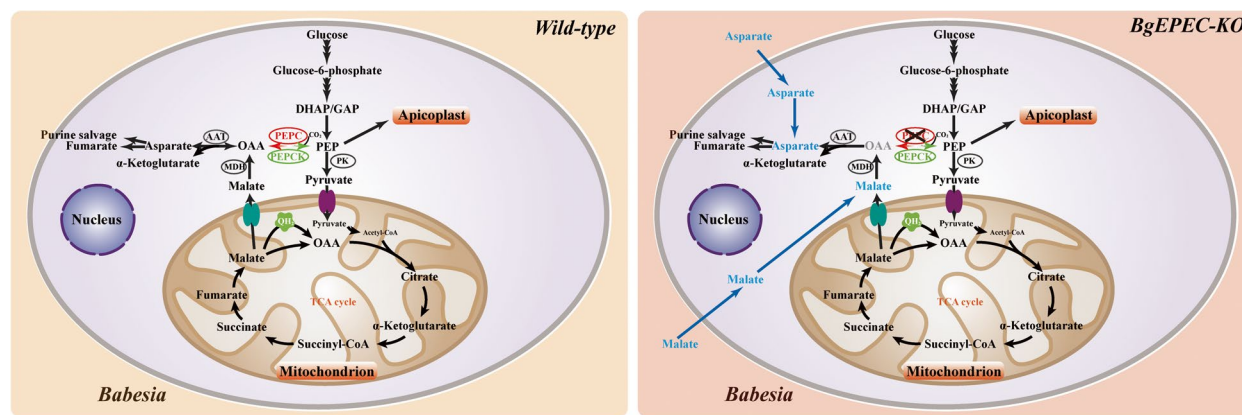
²Key Laboratory of Animal Epidemical Disease and Infectious Zoonoses, Ministry of Agriculture, Huazhong Agricultural University, Wuhan 430070, Hubei, China

³Key Laboratory of Preventive Veterinary Medicine in Hubei Province, Wuhan 430070, Hubei, China



© The Author(s) 2024. **Open Access** This article is licensed under a Creative Commons Attribution 4.0 International License, which permits use, sharing, adaptation, distribution and reproduction in any medium or format, as long as you give appropriate credit to the original author(s) and the source, provide a link to the Creative Commons licence, and indicate if changes were made. The images or other third party material in this article are included in the article's Creative Commons licence, unless indicated otherwise in a credit line to the material. If material is not included in the article's Creative Commons licence and your intended use is not permitted by statutory regulation or exceeds the permitted use, you will need to obtain permission directly from the copyright holder. To view a copy of this licence, visit <http://creativecommons.org/licenses/by/4.0/>. The Creative Commons Public Domain Dedication waiver (<http://creativecommons.org/publicdomain/zero/1.0/>) applies to the data made available in this article, unless otherwise stated in a credit line to the data.

Graphical Abstract



Introduction

During the intraerythrocyte development stage, *Babesia* undergoes maturation and replication, resulting in parasitemia, which is the main pathology of babesiosis (Lobo et al. 2012). This rapid development necessitates a constant supply of nutrients, primarily glucose, to fulfill the parasite's energy needs (Beri et al. 2023; Ohmori et al. 2004). In apicomplexan parasites, the majority of glucose is metabolized into pyruvate, which is then reduced to lactate and expelled from the parasite. Although *Babesia* possesses all the genes necessary for the tricarboxylic acid (TCA) cycle and most of those required for electron transport chain (ETC) enzymes (Brayton et al. 2007; Liu et al. 2023; Singh et al. 2023), it relies predominantly on cytoplasmic glycolysis during the erythrocyte stage of development. Mitochondrial oxidative phosphorylation plays a minimal role in ATP synthesis in *Babesia* at this stage.

Energy acquisition and metabolism are critical for the survival and proliferation of all living organisms, and glucose metabolism represents the primary pathway through which life forms obtain energy (Mulukutla et al. 2016). The major pathways of ATP production in most organisms include glycolysis, the TCA cycle, and β -oxidation (Fernie et al. 2004). Glycolysis involves the breakdown of six-carbon glucose molecules into two molecules of phosphoenolpyruvate (PEP) through a nine-step enzymatic process, ending with substrate-level phosphorylation catalyzed by pyruvate kinase (Romano and Conway 1996). This results in the production of two three-carbon pyruvate molecules, generating two molecules of ATP to fuel the energy needs of living organisms (Kresge et al. 2005). The fate of pyruvate varies among species and depends on oxygen availability. Under aerobic conditions, pyruvate is transported into the mitochondria, where it

undergoes oxidative decarboxylation by the pyruvate dehydrogenase complex to produce acetyl-CoA (DeColli et al. 2018). Acetyl-CoA then combines with OOA—a product of PEP—to initiate the TCA cycle and oxidative phosphorylation, ultimately yielding CO_2 , H_2O , and ATP to energize the organism (Arnold and Finley 2023). OOA, a crucial reactant in the TCA cycle, also serves as a significant source of malate, aspartate, and other substances, playing a vital role in the organism's material and energy metabolism.

Phosphoenolpyruvate carboxylase (PEPC) is a cytoplasmic enzyme present in a wide range of organisms, including plants, green algae, cyanobacteria, bacteria, archaea and protozoa (Izui et al. 2004; Storm et al. 2014). It catalyzes the conversion of bicarbonate (HCO_3^-) and PEP into 4-carbon oxaloacetic acid and inorganic phosphate (Pi) (Kai et al. 2003). This reaction plays a pivotal role in the carbon fixation processes observed in crasulacean acid metabolism (CAM) and C_4 organisms and in regulating the flux of the TCA cycle in bacteria and plants (Nimmo 2000).

The biological importance of PEPC has increasingly been recognized in various aspects of many eukaryotic cells, but its role in *Babesia* remains entirely unknown. The conversion of PEP to OOA, which is mediated by the PEPC enzyme, not only provides the necessary materials and energy for growth and survival but also plays a crucial role in CO_2 fixation for carbon metabolism. These findings suggest that PEPC could be a key factor for the growth and survival of *Babesia*. Given the pivotal role of the PEPC in glycolysis, identifying its function during the erythrocyte stage of *Babesia* and understanding its contributions to intermediate carbon metabolism and intracellular survival could significantly advance our knowledge of *Babesia*'s energy metabolism and lay the

groundwork for developing the PEPC as a potential drug or vaccine target aimed at regulating parasite metabolism. In this study, we aimed to elucidate the contributions of PEPC to the carbon metabolism and survival of *B. gibsoni* during development in erythrocytes.

Results

***B. gibsoni* genomes code for putative phosphoenolpyruvate carboxylase homologs**

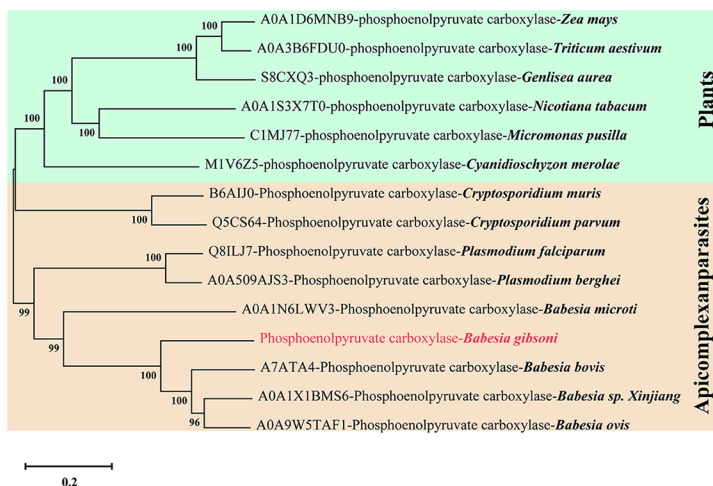
The reactions mediated by PEPC play crucial roles in several biochemical pathways, including the production of OOA, CO₂ fixation, recovery of purines, and the formation of glycolytic intermediates. Investigating PEPC further is essential for understanding the mechanism of energy metabolism in insects and for identifying potential drug targets. Initially, we discovered a gene in the *B. gibsoni* genome database that encodes a

putative PEPC comprising 958 amino acids with a conserved catalytic domain (Fig. 1A). We also searched for BgPEPC homologs in related apicomplexan parasites and compared apicomplexan PEPC with plant PEPC. All the sequences shared high sequence identity with BgPEPC and the typical PEPC domain. Phylogenetic analysis revealed clustering of apicomplexan PEPCs into one separate group, containing PEPCs from *Cryptosporidium*, *Plasmodium*, and *Babesia*, and another group containing plants and fungi (Fig. 1B). AlphaFold3 was employed to generate a homology model of the *B. gibsoni* PEPC protein. This shows that the function of the *B. gibsoni* PEPC is in good agreement with the equivalent in the PEPC of other apicomplexan parasites. The model revealed that the β -sheet structure within the active site cavity is similar to that observed in *Escherichia coli* and *Plasmodium* PEPC and is surrounded by an α -helix structure.

A



B



C

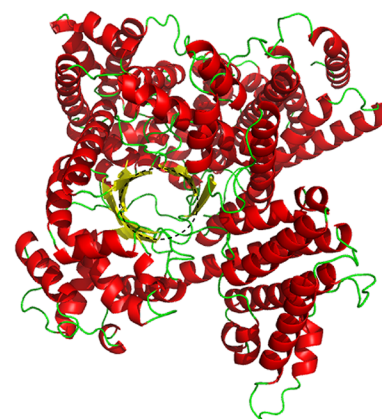


Fig. 1 Evolutionary analysis and multiple sequence alignment of PEPC proteins in different species. **A** Amino acid sequence comparison of PEPCs from different species. **B** Amino acid sequence evolutionary tree of PEPC in different species. Red represents the PEPC of *B. gibsoni*. **C** BgPEPC tertiary structure simulation via AlphaFold3. Red indicates a helix, yellow indicates a beta-sheet, and green indicates a loop. The black dashed line indicates the active site region

BgPEPC is expressed in asexual erythrocytic stages and localizes to the cytoplasm

To determine the expression and cellular localization of BgPEPC, we replaced the wild-type BgPEPC coding region with BgPEPC-3×Flag coding sequence in the *B. gibsoni* WH strain via a double-cross homologous recombination strategy. This involved utilizing the downstream coding sequence and the 3' UTR of BgPEPC as homologous arms to clone 3×Flag tags to its C-terminal end. Additionally, an eGFP fluorescent protein box driven by an actin promoter and a BSD drug selection marker box were employed as screening tags (Fig. 2A). The integrated parasites were identified through multiple drug selection cycles. To verify the correct integration of the pBS-BgPEPC-3×Flag construct into the parasite genome, cloned BgPEPC-3×Flag knock-in (BgPEPC-3×Flag) parasites were evaluated for replacement of the target gene via PCR, and the expression of the fusion protein was evaluated via western blotting. The wild-type coding region of the BgPEPC-3×Flag parasite was replaced with BgPEPC-3×Flag coding sequences. The knockin strain was amplified via gene-specific primers to confirm the integration of the knockin plasmid at its chromosomal site (Fig. 2B). Western blotting of the wild type (WT) and BgPEPC-3×Flag parasite crude proteins revealed the reactivity of the BgPEPC-3×Flag fusion protein at the expected 105 kDa band via the anti-Flag antibody (Fig. 2C). An indirect immunofluorescence assay (IFA) using an anti-Flag antibody revealed strong fluorescence signals in all morphologies of BgPEPC-3×Flag parasites. Notably, the signals were predominantly localized in the cytoplasm of the parasites (Fig. 2D).

BgPEPC can be knocked out only with exogenous malate supplementation

To analyze the contribution of BgPEPC to parasite development and life cycle progression, we attempted to knock out the BgPEPC gene in BgPEPC-3×Flag parasites via a double-cross homologous recombination method. The donor plasmid pBluescript, which contains the fluorescent protein mCherry and drug selection marker puromycin boxes driven by expression with the Bgef1a-B promoter, along with the Bgef1a 5' and 3' UTR regions of the BgPEPC genes as homologous arms, was transfected into BgPEPC-3×Flag parasites (Fig. 3A). Despite several attempts, the pBS-ΔPEPC plasmid failed to integrate into the correct gene locus consistently, indicating the potential importance or indispensability of the PEPC gene for parasite survival. It is hypothesized that the deletion of the PEPC gene disrupts downstream metabolite production, leading to parasite death and preventing the acquisition of a correctly integrated gene deletion strain. Given that studies have demonstrated the feasibility of knocking

out the malaria parasite PEPC through malate supplementation in culture medium, this study attempted to add malic acid, a downstream metabolite, during the construction of BgPEPC knockout parasites. To ensure that malate does not adversely affect Babesia growth, the effects of various malate concentrations on WT parasites were examined to determine the appropriate concentration. Compared with that of the medium without malate, the infection rate of the WT parasite decreased with increasing malate concentration over three consecutive cycles, whereas no significant difference in the infestation rate was detected with 5 mM malate or lower malate concentrations. Consequently, 5 mM malate was added to the medium when BgPEPC gene knockout was performed (Fig. 3B). After puromycin-driven selection, PCR confirmed the presence of a correctly integrated knockout parasite (Fig. 3C). Limiting dilution cloning of the transfected parasite population resulted in the isolation of 3 parasite clones (C9, E9, and G4), and the gene deletion was confirmed by diagnostic PCR, which revealed the expected alteration of the genomic DNA (Fig. 3D). Complete knockout of the BgPEPC-3×Flag-Rap1 3'U-Actin Pro-eGFP/BSL sequence and expression of the mCherry/PAC protein were verified via western blotting of a cloned recombinant line (ΔBgPEPC-C9) (Fig. 3E, F). IFA revealed the mCherry signal observed in the ΔBgPEPC-C9 parasites, and no eGFP signal was detected, confirming the successful knockout of the BgPEPC coding sequence (Fig. 3G).

BgPEPC is important for asexual erythrocyte stage development

To investigate the impact of PEPC deficiency on the parasite, this study monitored the infection rate over three consecutive subcultures, comparing the ΔBgPEPC, BgPEPC-3×Flag, and WT parasites (Fig. 4A). The optimal concentration of malate was detected by PPE in three subcultures of ΔBgPEPC parasites. A minimum of 1 mM malate was crucial for effectively knocking out BgPEPC, and this concentration was subsequently used for phenotype analysis (Fig. 4B). The absence of PEPC did not influence the growth pattern of the parasite, with no significant difference in the proportion of parasites with different morphologies among the ΔBgPEPC(+ Malate), BgPEPC-3×Flag and WT strains ($p > 0.01$). However, a lower proportion of double rings was observed in the ΔBgPEPC strain without malate than in the ΔBgPEPC strains with 1 mM malate, BgPEPC-3×Flag and WT strains ($p < 0.01$) (Fig. 4C). Continuous monitoring across three subcultures revealed that parasites could sustain growth without PEPC, albeit at a significantly reduced rate compared with the BgPEPC-3×Flag and WT parasites (Fig. 4D). Therefore, although BgPEPC is not

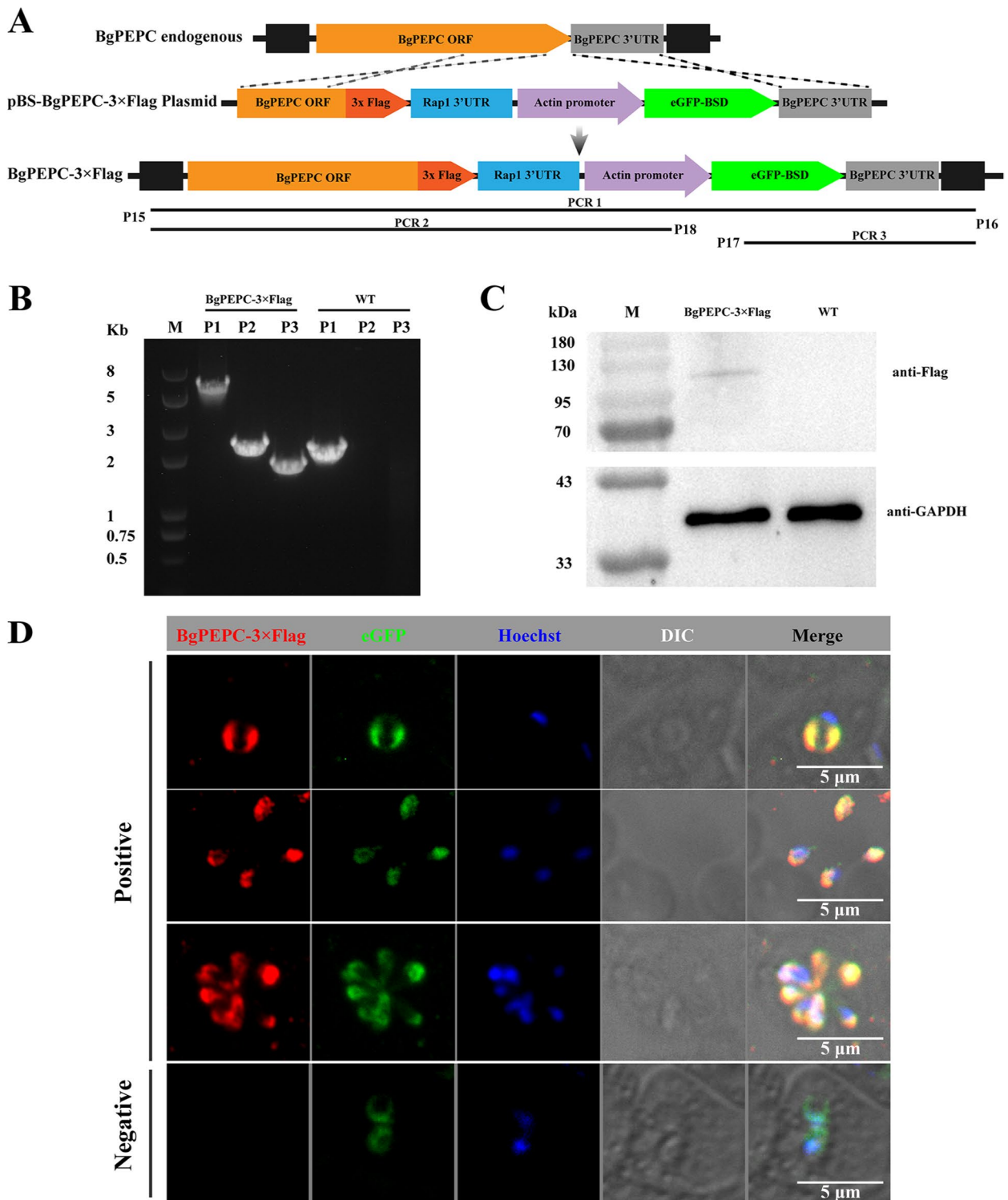


Fig. 2 Generation of the BgPEPC-3×Flag parasite. **A** Schematic representation of the integration of the transfected plasmid DNA into the endogenous BgPEPC locus, generating the integration locus. **B** The ethidium bromide-stained agarose gel shows PCR products amplified from the genomic DNA of wild-type (WT) and BgPEPC-3×Flag parasites via the indicated primer sets. **C** Lysates of wild-type *B. gibsoni* (WT) and BgPEPC-3×Flag parasites were assessed for the expression of BgPEPC/3×Flag via western blotting. **D** The ring and trophozoite stages of BgPEPC-3×Flag parasites were assessed for the localization of BgPEPC/3×Flag parasites via indirect immunofluorescence assay (IFA). All parasites were imaged using the PLYMPUS FARME_BX63 fluorescence microscope with a 100×numerical-aperture (NA) oil objective

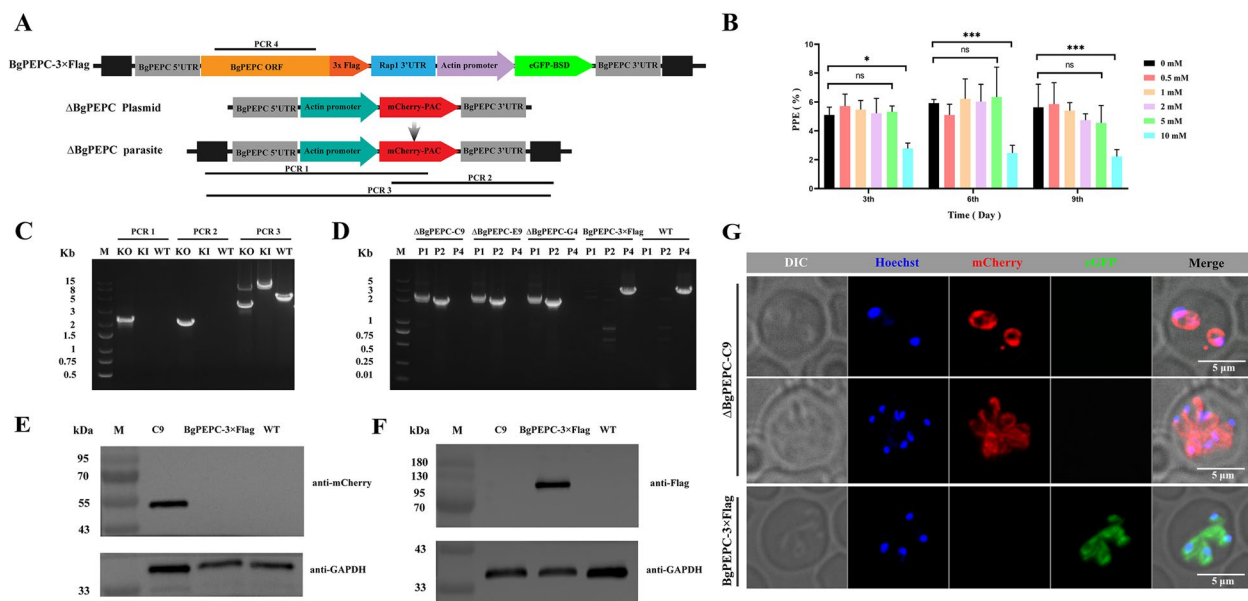


Fig. 3 Generation of BgPEPC knockout parasites. **A** Schematic diagram showing the integration of the transfected plasmid DNA into the endogenous BgPEPC locus, generating the predicted integration event. **B** Wild-type parasites were cultured for three consecutive cycles with different concentrations of malate, each spanning approximately 72 h. **C** The ethidium bromide-stained agarose gel shows PCR products amplified from the genomic DNA of the wild-type (WT), BgPEPC-3 × Flag (KI) and ΔBgPEPC (KO) parasites via locus-specific primers. **D** The ethidium bromide-stained agarose gel shows PCR products amplified from three clones of ΔBgPEPC (C9, E9 and G4), BgPEPC-3 × Flag and wild-type (WT) parasites via locus-specific primers. **E** Lysates of wild-type *B. gibsoni* (WT), BgPEPC-3 × Flag and ΔBgPEPC (C9) parasites were assessed for the expression of mCherry/PAC via western blotting. **F** Lysates of wild-type *B. gibsoni* (WT), BgPEPC-3 × Flag and ΔBgPEPC (C9) parasites were assessed for the expression of BgPEPC/Flag via western blotting. **G** The expression of mCherry/PAC and BgPEPC/Flag was evaluated via IFA with anti-mCherry and anti-Flag antibodies. All parasites were imaged using the PLYMPUS FARME_BX63 fluorescence microscope with a 100 × numerical-aperture (NA) oil objective

essential for the growth and multiplication of blood-stage *B. gibsoni* in vitro, the absence of BgPEPC expression affects parasite growth.

To determine whether other downstream metabolites compensate for the absence of PEPC, we introduced 1 mM of various metabolites—OAA, citrate, aspartate, pyruvate, glycerol, and malate—into the culture medium. The infection rates of the ΔBgPEPC, BgPEPC-3 × Flag, and WT strains were then assessed via a medium without additional metabolites as the control. The findings revealed that the external addition of aspartate and malate supported the growth of the knockout strains, with malate showing the most significant effect. This enhancement by malate could be attributed to its role as an additional pathway for OAA synthesis, filling the metabolic gap left by gene deletion (Fig. 4E).

The absence of BgPEPC increases the sensitivity to L-cycloserine

To investigate the mechanisms underlying the enhanced survival of the ΔBgPEPC strains, this study assessed their susceptibility to metabolic inhibitors. Triazamidine, also

known for its commercial name Benir, is an aromatic diamidine compound commonly used as an antitrypanosomic drug in clinical settings. It inhibits parasites such as *Babesia* by targeting DNA replication and mitochondrial energy metabolism processes (Fig. 5A). Cycloserine acts as a competitive inhibitor of phosphopyridoxal-dependent enzymes, such as aspartate aminotransferase (AAT), and has potent antiparasitic effects (Fig. 5B). The IC_{50} values for triazamidine were 5.84 nM for the wild-type strain and 5.22 nM for the BgPEPC-3 × Flag strains, whereas for the ΔBgPEPC strains, the IC_{50} values significantly decreased to 1.63 nM and 1.36 nM, respectively (Fig. 5C). This increased drug sensitivity in gene-knockout strains may result from triazamidine impairing the glycolysis process and mitochondrial function, a vulnerability not mitigated by malate supplementation. These findings suggest that the target of triazamidine cannot be compensated for by malate alone. Furthermore, the IC_{50} values for L-cycloserine varied significantly among the strains, with the ΔBgPEPC strains showing heightened sensitivity (WT IC_{50} at 16 μM, BgPEPC-3 × Flag at 12.27 μM, and ΔBgPEPC at 6.589 μM). When the

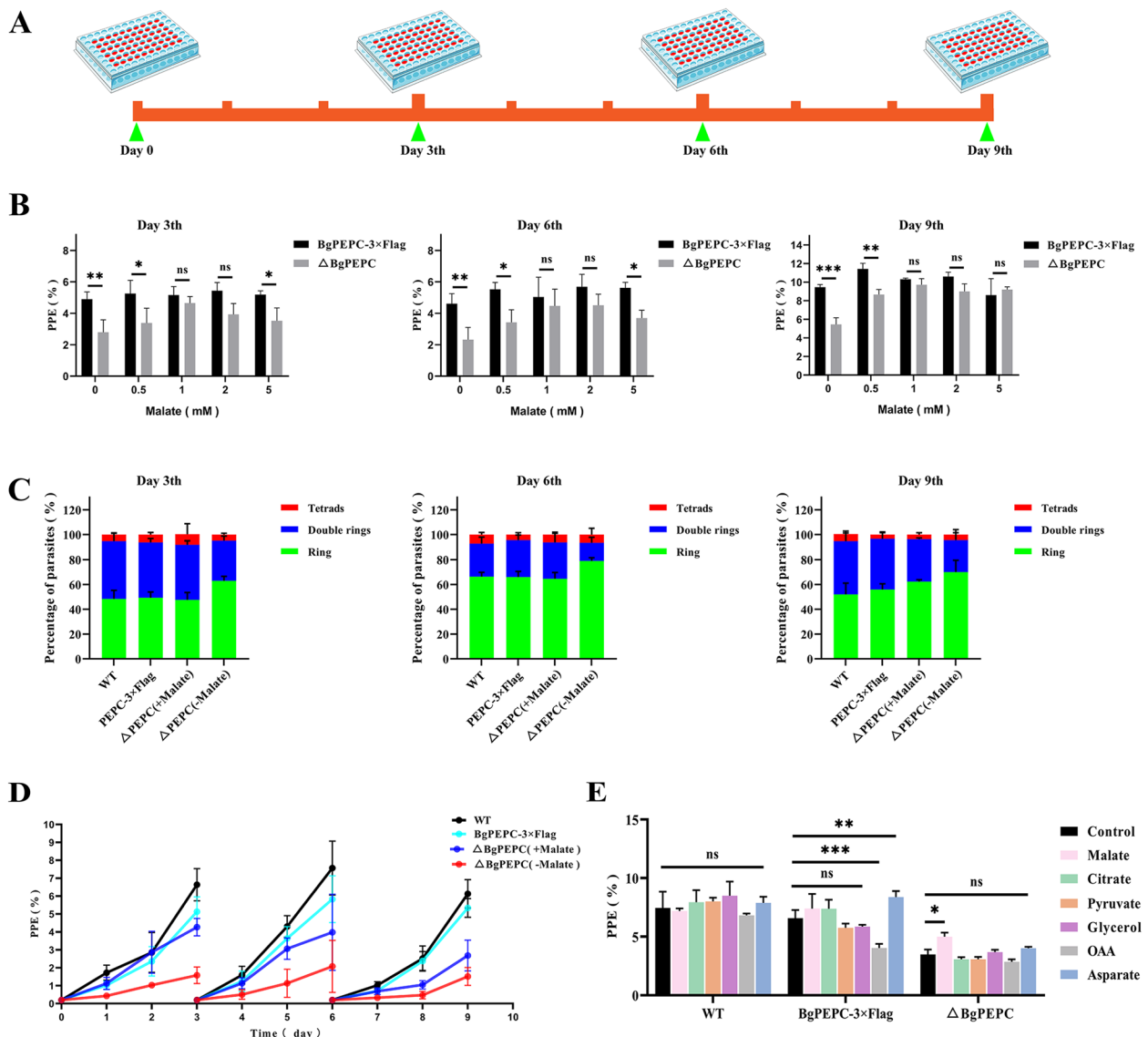


Fig. 4 Phenotypic analysis of the Δ BgPEPC parasite. **A** Schematic diagram of the phenotypic analysis. The green solid triangle indicates the time of each subculture with 0.2% primary parasitemia. **B** Wild-type and Δ BgPEPC parasites were cultured for three consecutive cycles with different concentrations of malate (0, 0.5, 1, 2, or 5 mM/mL). **C** Wild-type, BgPEPC-3 \times Flag, Δ BgPEPC (without malate) and Δ BgPEPC (with 1 mM malate) parasites were cultured for three consecutive cycles, and the proportions of different morphologies were determined at the end of each cycle. **D** Wild-type, BgPEPC-3 \times Flag, Δ BgPEPC (without malate) and Δ BgPEPC (with 1 mM/mL malate) parasites were cultured for three consecutive cycles, and parasitemia was determined at the beginning and end of each cycle. **E** Parasitaemia of wild-type, BgPEPC-3 \times Flag and Δ BgPEPC parasites that were cultured for one cycle with the addition of different metabolites (1 mM)

Δ BgPEPC strains were cultured with 1 mM malic acid, this sensitivity was partially reversed (the IC_{50} increased to 13.55 μ M), highlighting the effect of PEPC gene deletion on reducing the production of its product, OAA (Fig. 5D). Consequently, this reduction leads to increased sensitivity to competitive inhibitors such as L-cycloserine, as it impacts the synthesis of aspartic acid and exacerbates vulnerability to such inhibitors.

Discussion

Metabolism, which involves both material and energy metabolism, is a fundamental characteristic of life and is essential for the survival and multiplication of all organisms, including parasites. For example, adenosine triphosphate (ATP) is generated through glycolysis and oxidative phosphorylation to sustain growth. In the study of the energy metabolism mechanism in Apicomplexan

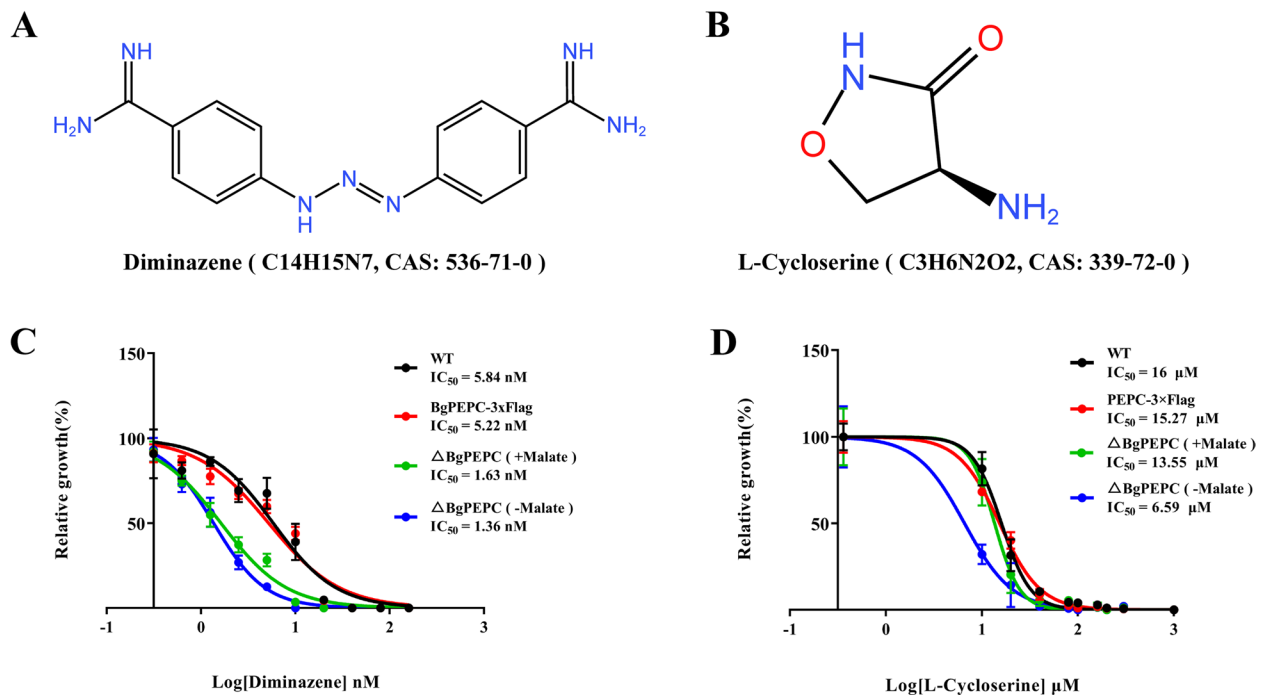


Fig. 5 Susceptibility analysis of parasites to metabolic inhibitors. **A** Molecular formula of Diminazene. **B** Molecular examples of L-cycloserine. **C** Drug sensitivity of Diminazene Aceturate to three strains of *B. gibsoni* in routine medium and malate supplementation. **D** Drug sensitivity of L-cycloserine to three strains of *B. gibsoni* in routine medium supplemented with malate

parasites, these organisms often lack key enzymes of the TCA cycle. Consequently, these bacteria primarily rely on glycolysis under anaerobic conditions for their energy needs. However, recent research has revealed that the TCA cycle contributes to the energy metabolism of Apicomplexan parasites in ways that are distinct from those in mammals. It supports glycolysis by providing the energy or intermediate metabolites necessary for the parasitic life of Apicomplexan parasites.

The metabolic linkage between glycolysis and the TCA cycle is facilitated by intermediates such as OOA and pyruvate. OAA and the glycolytic metabolite PPE can be interconverted, with the enzymes phosphoenolpyruvate carboxykinase (PEPCK) (Hayward 2000; Nitzsche et al. 2017) and PEPC (Barazandeh et al. 2021; Storm et al. 2014) mediating the reversible reaction. PEPC, a cytoplasmic enzyme, catalyzes the beta-carboxylation of PEP in the presence of HCO_3^- (generated from CO_2 by carbonic anhydrase) and produces OAA and inorganic phosphate (Pi), suggesting that PEPC plays a pivotal role in carbon metabolism in *Babesia* by facilitating carbon dioxide fixation. The production of OAA and subsequently aspartate by the enzyme underscores its importance in sustaining the vital metabolic functions necessary for parasite growth. Motif and domain analyses underscored the high conservation of the PEPC gene

across *Babesia* species, akin to those observed in *Plasmodium* and *Cryptosporidium*.

The knockout of the PEPC gene is feasible only with the supplementation of exogenous malate, underscoring the crucial role of PEPC in synthesizing malate via OAA for key metabolic reactions. The severe growth defects observed in the ΔBgPEPC strains without malate supplementation and the partial rescue caused by the addition of malate further validated this role. Similar patterns are observed in PEPC-deficient *Plasmodium falciparum*, which also presents significant growth challenges but can be partially alleviated by the addition of high concentrations of fumarate or malate (Storm et al. 2014). PEPC catalyzes the conversion of PEP and HCO_3^- into OAA, a pivotal intermediate in the TCA cycle. OAA then combines with acetyl-CoA under the action of citrate synthase to produce citric acid (Koendjiharie et al. 2021). The survival of ΔBgPEPC strains without supplemental malate may rely on these metabolites being sourced from the TCA cycle, although this is insufficient to fully compensate for the severe growth defects observed.

Within the parasite, OAA generated by PEPC is transformed into aspartate and α -ketoglutarate by AAT (Berger et al. 2001; Holecek 2023). As an α -amino acid, aspartate is an important precursor for protein/purine/pyrimidine biosynthetics (Moffatt and Ashihara

2002). The ability to offset the reduced production of OAA by supplementing aspartate suggests the importance of aspartate for parasite survival. Purine and pyrimidine are joined by phosphate bonds to form the backbone of nucleic acids to form the basic structure of DNA and RNA. The proportion of tetrad forms in the Δ BgPEPC strains decreased without malate supplementation and returned to normal levels with supplementation, illustrating the impact of aspartate on parasite differentiation. Moreover, attempts to compensate for diminished parasite growth due to reduced OAA production by adding exogenous OAA to the medium may fail because the externally supplied OAA might not be effectively assimilated by the parasite. It is hypothesized that the addition of pyruvate and glycerol may not ameliorate growth defects resulting from PEPC knockdown. Lactate dehydrogenase (LDH) typically facilitates the conversion of pyruvate into lactate and acetyl-CoA in other *Babesia* species (Yu et al. 2021), but LDH has not been identified in *B. gibsoni*, indicating the absence of this metabolic pathway or the involvement of another enzyme in this process. Although glycerol can be converted into dihydroxyacetone phosphate and subsequently enter glycolysis or gluconeogenesis to fuel cellular metabolism (Ginsburg 2010; Kovarova et al. 2018), the PEPC knockout strain showed no positive response to glycerol supplementation, possibly because ATP acquisition in glucose pathways was unaffected. These findings suggest that the metabolic adjustments required to overcome the deficiencies caused by PEPC knockout are not met by glycerol supplementation alone.

L-cycloserine acts as a competitive inhibitor of phosphopyridoxal-dependent enzymes, such as AATs (Janski and Cornell 1981; Nakamura et al. 2022). AAT facilitates the mutual conversion of oxaloacetic acid and glutamic acid into aspartic acid and alpha-ketoglutaric acid (Kirsch et al. 1984). The heightened sensitivity to L-cycloserine observed in strains in which the PEPC gene was knocked out suggests that the absence of PEPC may reduce aspartate production. In addition, there is a potential impact on the glycolytic reaction and the malate shuttle system, which are associated with PEPC products. We explored the differences in the sensitivity of PEPC-knockout strains and control strains to diminazene aceturate (DA), the primary mode of action of which includes the inhibition of the glycolysis pathway and mitochondrial respiratory activity (Wickramasekara Rajapakshage et al. 2012). Our findings indicate that sensitivity to DA is increased in BgPEPC knockout strains. However, supplementation with malate did not significantly mitigate this sensitivity, suggesting that malic acid supplementation alone cannot compensate for the specific biochemical deficits induced by the loss of BgPEPC.

Conclusions

In summary, our research into metabolic modifications in BgPEPC knockout strains provides an enhanced understanding and fresh insights into the critical roles of *Babesia* PEPC. PEPC catalyzes the conversion of PEP into OAA, which subsequently forms aspartate and a-ketoglutarate. Aspartate serves as a precursor in the biosynthesis of proteins, purines, and pyrimidines, making it a crucial component for DNA synthesis and parasite replication. Malate, a key intermediate in the TCA cycle, can be transported from the mitochondria to the cytoplasm of the parasite via malate shuttling to produce OOA, partially compensating for the disrupted OAA production caused by the absence of BgPEPC. Our findings suggest that disrupting these metabolic pathways could significantly impair parasite viability within host erythrocytes, highlighting PEPC as a potential drug target for therapeutic intervention in babesiosis.

Methods

Analysis of amino acid sequences

The PlasmoDB (<http://PlasmoDB.org>) and NCBI (<https://www.ncbi.nlm.nih.gov/>) databases were used to acquire amino acid sequences, and the BLAST tool was used to search for homologs. The InterProScan (<https://www.ebi.ac.uk/interpro/>) database was used for domain identification. Sequence alignment was performed via the Clustal Omega Multiple Sequence Alignment Tool (<https://www.ebi.ac.uk/Tools/msa/clustalo/>). AlphaFold3 (<https://alphafoldserver.com/>) was used to model the structure of the BgPEPC protein, and PyMOL 3.0 (<https://www.pymol.org/>) was used to visualize the results.

Parasite culture

Parasites were cultured in VP-SFM supplemented with Albimax I (Gibco) and 2.5% dog serum as described previously (Li et al. 2023). In brief, each culture started with 0.5% parasitemia with 10% hematocrit (HCT), and the medium was changed every 24 h by discarding the 90% culture supernatant and adding an equivalent amount of fresh medium. The subculture was initiated by diluting parasitemia to 0.5% in the new well at 72 h. Dog serum was isolated from blood collected from healthy beagle dogs. Red blood cells (RBCs) were aseptically collected in sterile blood collection tubes containing anticoagulants. The RBCs were then washed three times with RPMI-1640 medium or MAP RBC preservation solution. All the cultures were maintained in a CO₂ incubator at 37°C.

Plasmid construction

The pBS-BgPEPC-3×Flag plasmid contains two 750 bp homologous regions to the 3' end (stop codon

not included, P1/P2), the 3' UTR of the BgPEPC gene (P3/P4), and the 3×Flag- RAP1 3' UTR-action promoter- eGFP/BSD fragment (P5/P6). The pBS-BgPEPC-KO plasmid was prepared by amplifying the 5' UTR (750 bp) and 3' UTR (750 bp) of the BgPEPC gene via the primers P7/P8 and P9/P10; the efla-B promoter fragment; and the mCherry-PAC fragment, which was amplified from the pBS-mCherry-PAC plasmid via the primers P11/P12 and P13/P14. All primers included homologous regions used for ligation-independent fragments. All PCR amplifications were performed with high-fidelity polymerase (Vazyme) following the recommended protocols. All sequences of primers used in this study are provided in Table S1.

Transfections and isolation of clonal cell lines

To generate BgPEPC-3×Flag mutants, *B. gibsoni* WH strains were transfected with the pBS-BgPEPC-3×Flag plasmid. Transfections and drug selection were performed as described previously (Li et al. 2024). In brief, approximately 10⁸ parasites were resuspended in 100 µL of Cytomix electrotransfer buffer containing 50 µg of the linearized plasmid. A Bio-Rad electroporator (Bio-Rad, model number: Gene Pulser Xcell) was used for electroporation with two electroporation pulses under the following conditions: 1200 V, 200 Ω, and 25 µF. Twenty-four hours posttransfection, the growth medium was supplemented with blasticidin S or puromycin (Solarbio). Individual eGFP-positive cells from a single transfection were cloned and inserted into 96-well plates via the limiting dilution method. To determine whether homologous recombination occurs specifically at the targeted site, PCR primers for BgPEPC, both inside and outside the inserted guide 5' and 3' sequences, were designed, and the amplicon was sequenced (Table S1). Parasite genomic DNA for PCR amplification was extracted via a TIANamp Genomic DNA Kit (TIANGEN), and PCR analysis was performed with 2×Rapid Taq Master Mix (Vazyme). After PCR identification was performed for clones G3 and E4, the parasites were transferred to media containing 4 mM BSD to facilitate optimal growth. The BgPEPC knockout (KO) parasite was generated by transfecting BgPEPC-3×Flag G3 parasites with the pBS-BgPEPC-KO plasmid. Parasites expressing these PAC constructs were selected via the use of 2 nM puromycin (Sigma). Individual mCherry-positive cells were cloned and inserted into 96-well plates via the limiting dilution method as previously described.

Western blotting

Parasite pellets were isolated via cold 0.04% saponin (Sigma) in 1×PBS for 10 min. The antibodies used for

this study were as follows: rabbit anti-Flag (1:2000), rabbit anti-GFP (1:2000), rabbit anti-mCherry (1:2000), and mouse anti-GAPDH (1:2000). The secondary antibodies used were goat anti-rabbit IgG and goat anti-mouse IgG (1:5000). The proteins were imaged via western blotting via an Odyssey infrared imaging system. The polyacrylamide gels used in this study were prepared via precast gradient gels (4–20%, from Bio-Rad).

Live fluorescence microscopy

To visualize BgPEPC-3×Flag live parasites, 100 µL of parasite culture was pelleted, and the supernatant was removed. The parasites were resuspended in 100 µL of PBS with 5 µM Hoechst 33342 and incubated at 37°C for 10 min. The parasites were then pelleted again, and 90% of the PBS was removed. The parasites were resuspended in the remaining PBS, and 1 µL of the culture was placed on a glass slide and covered with a coverslip. The cells were imaged via an OLYMPUS FARME_BX63 fluorescence microscope with a 100×numerical-aperture (NA) oil objective.

Immunofluorescence (IFA) assays and image processing

IFAs were performed as described previously. Briefly, thin blood smears were fixed with 4% paraformaldehyde and then permeabilized with 0.1% (v/v) Triton X-100. After blocking with 3% BSA, the smears were incubated with primary antibodies (rabbit anti-Flag, rabbit anti-GFP, and rabbit anti-mCherry) at 1:500 dilutions. After three washes with PBS, the parasites were incubated with secondary antibodies (Alexa Fluor-conjugated goat anti-rabbit 488, Alexa Fluor-conjugated goat anti-rabbit 594, Alexa Fluor-conjugated goat anti-mouse 499, and Alexa Fluor-conjugated goat anti-mouse 594) at 1:500 dilutions and washed with PBS three times. All parasites were incubated with PBS containing 1 µg/mL Hoechst and imaged via an OLYMPUS FARME_BX63 fluorescence microscope with a 100×numerical-aperture (NA) oil objective.

Survival assay and in vitro drug susceptibility assays

The survival assay method was performed on *B. gibsoni* WH, BgPEPC-3×Flag, and BgPEPC-KO parasites as described previously (Li et al. 2023). In brief, parasites at 10% final HCT and 0.5% parasitemia in a total volume of 100 µL were incubated at 37°C in a 96-well plate for 72 h. Parasitemia was determined every 24 h via Giemsa-stained blood smears, with 3000 RBCs counted on each slide. All the statistical analyses were carried out via GraphPad Prism 8.

Inhibitors were used to perform in vitro drug susceptibility tests in standard cultures of *B. gibsoni* blood

samples. For testing *B. gibsoni* inhibition, parasites were adjusted to 0.5% parasitemia and 10% hematocrit (100 μ L total in a 96-well plate) at 37°C for 72 h with different concentrations of drugs for drug susceptibility assays, parasitemia, and developmental stage of parasites were analyzed via Giemsa-stained blood smears, with 3000 RBCs counted on each slide. The half-maximal inhibitory concentration (IC50) was estimated via a nonlinear regression model implemented in GraphPad Prism 8. Two-way ANOVA with Dunnett's multiple comparison test was used for statistical analysis (P value $***p < 0.0001$, $**p < 0.001$, $*p < 0.01$).

Abbreviations

AAT	Aspartate aminotransferase
ATP	Adenosine triphosphate
CAM	Crassulacean acid metabolism
DA	Diminazene aceturate
ETC	Electron transport chain
HCT	Hematocrit
IFA	Immunofluorescence assay
KO	Knock out
LDH	Lactate dehydrogenase
OAA	Oxaloacetic acid
PEP	Phosphoenolpyruvate
PEPC	Phosphoenolpyruvate carboxylase
PEPCK	Phosphoenolpyruvate carboxykinase
TCA	Tricarboxylic acid
WT	Wild-type

Supplementary Information

The online version contains supplementary material available at <https://doi.org/10.1186/s44149-024-00148-5>.

Supplementary Material 1.

Authors' contributions

J.-L. Z. and L. H. designed the experiments; D.-F. L., L.-N. W., Y.-D. B., Y.-X. Y., X.-A. G., X. L., and F.-J. L. performed the experiments; D.-F. L., and S. W. analyzed the data and wrote the manuscript.

Funding

This work was supported by the National Natural Science Foundation of China (32172879), the National Key Research and Development Program of China (2022YFD1801700 and 2022YFD1800200), and the Top-notch Young Talent Supporting Program to Lan He. Additionally, funding was obtained from the Fundamental Research Funds for the Central Universities (2662020DKPY016 and 2262022DKYJ001).

Data availability

The data used to support the findings of this study are available from the corresponding author upon request.

Declarations

Competing interests

The authors declare that they have no conflicts of interest.

Received: 20 September 2024 Accepted: 30 October 2024

Published online: 04 December 2024

References

- Arnold, P.K., and L.W.S. Finley. 2023. Regulation and function of the mammalian tricarboxylic acid cycle. *The Journal of Biological Chemistry* 299 (2): 102838. <https://doi.org/10.1016/j.jbc.2022.102838>.
- Barazandeh, A.F., Z.R. Mou, N. Ikeogu, E.M. Mejia, C.A. Edechi, W.W. Zhang, J. Alizadeh, G.M. Hatch, S. Ghavami, G. Matlashewski, et al. 2021. The phosphoenolpyruvate carboxykinase is a key metabolic enzyme and critical virulence factor of *Leishmania major*. *Journal of Immunology* 206 (5): 1013–1026. <https://doi.org/10.4049/jimmunol.2000517>.
- Berger, L.C., J. Wilson, P. Wood, and B.J. Berger. 2001. Methionine regeneration and aspartate aminotransferase in parasitic protozoa. *Journal of Bacteriology* 183 (15): 4421–4434. <https://doi.org/10.1128/JB.183.15.4421-4434.2001>.
- Beri, D., M. Singh, M. Rodriguez, N. Goyal, G. Rasquinha, Y. Liu, X. An, K. Yazdankhsh, and C.A. Lobo. 2023. Global metabolomic profiling of host red blood cells infected with *Babesia divergens* reveals novel antiparasitic target pathways. *Microbiology Spectrum* 11 (2): e0468822. <https://doi.org/10.1128/spectrum.04688-22>.
- Brayton, K.A., A.O. Lau, D.R. Herndon, L. Hannick, L.S. Kappmeyer, S.J. Berens, S.L. Bidwell, W.C. Brown, J. Crabtree, D. Fadrosch, et al. 2007. Genome sequence of *Babesia bovis* and comparative analysis of apicomplexan hemoprotozoa. *PLoS Pathogen* 3 (10): 1401–1413. <https://doi.org/10.1371/journal.ppat.0030148>.
- DeColli, A.A., N.S. Nemeria, A. Majumdar, G.J. Gerfen, F. Jordan, and C.L. Freel Meyers. 2018. Oxidative decarboxylation of pyruvate by 1-deoxy-d-xulose 5-phosphate synthase, a central metabolic enzyme in bacteria. *The Journal of Biological Chemistry* 293 (28): 10857–10869. <https://doi.org/10.1074/jbc.RA118.001980>.
- Fernie, A.R., F. Carrari, and L.J. Sweetlove. 2004. Respiratory metabolism: Glycolysis, the TCA cycle and mitochondrial electron transport. *Current Opinion in Plant Biology* 7 (3): 254–261. <https://doi.org/10.1016/j.pbi.2004.03.007>.
- Ginsburg, H. 2010. Metabolism: Malaria parasite stands out. *Nature* 466 (7307): 702–703. <https://doi.org/10.1038/466702a>.
- Hayward, R.E. 2000. *Plasmodium falciparum* phosphoenolpyruvate carboxykinase is developmentally regulated in gametocytes. *Molecular and Biochemical Parasitology* 107 (2): 227–240. [https://doi.org/10.1016/S0166-6851\(00\)00191-2](https://doi.org/10.1016/S0166-6851(00)00191-2).
- Holecck, M., 2023. Roles of malate and aspartate in gluconeogenesis in various physiological and pathological states. *Metabolism: clinical and experimental* 145, 155614. <https://doi.org/10.1016/j.metabol.2023.155614>
- Izui, K., H. Matsumura, T. Furumoto, and Y. Kai. 2004. Phosphoenolpyruvate carboxylase: A new era of structural biology. *Annual Review of Plant Biology* 55: 69–84. <https://doi.org/10.1146/annurev.arplant.55.031903.141619>.
- Janski, A.M., and N.W. Cornell. 1981. Inhibition by cycloserine of mitochondrial and cytosolic aspartate aminotransferase in isolated rat hepatocytes. *The Biochemical Journal* 194 (3): 1027–1030. <https://doi.org/10.1042/bj1941027>.
- Kai, Y., H. Matsumura, and K. Izui. 2003. Phosphoenolpyruvate carboxylase: Three-dimensional structure and molecular mechanisms. *Archives of Biochemistry and Biophysics* 414 (2): 170–179. [https://doi.org/10.1016/S0003-9861\(03\)00170-x](https://doi.org/10.1016/S0003-9861(03)00170-x).
- Kirsch, J.F., G. Eichele, G.C. Ford, M.G. Vincent, J.N. Jansonius, H. Gehring, and P. Christen. 1984. Mechanism of action of aspartate aminotransferase proposed on the basis of its spatial structure. *Journal of Molecular Biology* 174 (3): 497–525. [https://doi.org/10.1016/0022-2836\(84\)90333-4](https://doi.org/10.1016/0022-2836(84)90333-4).
- Koendjibarie, J.G., van Kranenburg, R., Kengen, S.W.M., 2021. The PEP-pyruvate-oxaloacetate node: variation at the heart of metabolism. *FEMS microbiology reviews* 45(3), fuaa061. <https://doi.org/10.1093/femsre/fuua061>
- Kovarova, J., R. Nagar, J. Faria, M.A.J. Ferguson, M.P. Barrett, and D. Horn. 2018. Gluconeogenesis using glycerol as a substrate in bloodstream-form *Trypanosoma brucei*. *PLoS Pathogens* 14 (12): e1007475. <https://doi.org/10.1371/journal.ppat.1007475>.
- Kresge, N., R.D. Simoni, and R.L. Hill. 2005. Otto Fritz Meyerhof and the elucidation of the glycolytic pathway. *The Journal of Biological Chemistry* 280 (4): e3. [https://doi.org/10.1016/S0021-9258\(20\)76366-0](https://doi.org/10.1016/S0021-9258(20)76366-0).
- Li, D., L. Wang, X. Guan, S. Wang, Q. Liu, F. Chen, Y. Zheng, L. He, and J. Zhao. 2023. Establishment of continuous in vitro culture of *Babesia gibsoni* by using VP-SFM medium with low-concentration serum. *Microbiology Spectrum* 11 (3): e0025823. <https://doi.org/10.1128/spectrum.00258-23>.
- Li, D., S. Wang, X. Guan, Y. Bai, J. Zhao, and L. He. 2024. In vitro culture and genetic modification of *Babesia gibsoni*. *Decoding Infection and Transmission* 2: 100019. <https://doi.org/10.1016/j.dcit.2024.100019>.

- Liu, Q., X.A. Guan, D.F. Li, Y.X. Zheng, S. Wang, X.N. Xuan, J.L. Zhao, and L. He. 2023. *Babesia gibsoni* whole-genome sequencing, assembling, annotation, and comparative analysis. *Microbiology Spectrum* 11 (4): e0072123. <https://doi.org/10.1128/spectrum.00721-23>.
- Lobo, C.A., M. Rodriguez, and J.R. Cursino-Santos. 2012. *Babesia* and red cell invasion. *Current Opinion in Hematology* 19 (3): 170–175. <https://doi.org/10.1097/MOH.0b013e328352245a>.
- Moffatt, B.A., and H. Ashihara. 2002. Purine and pyrimidine nucleotide synthesis and metabolism. *The Arabidopsis Book* 1: e0018. <https://doi.org/10.1199/tab.0018>.
- Mulukutla, B.C., A. Yongky, T. Le, D.G. Mashek, and W.S. Hu. 2016. Regulation of glucose metabolism - a perspective from cell bioprocessing. *Trends in Biotechnology* 34 (8): 638–651. <https://doi.org/10.1016/j.tibtech.2016.04.012>.
- Nakamura, R., S. Ogawa, Y. Takahashi, and T. Fujishiro. 2022. Cycloserine enantiomers inhibit PLP-dependent cysteine desulfurase SufS via distinct mechanisms. *The FEBS Journal* 289 (19): 5947–5970. <https://doi.org/10.1111/febs.16455>.
- Nimmo, H.G. 2000. The regulation of phosphoenolpyruvate carboxylase in CAM plants. *Trends in Plant Science* 5 (2): 75–80. [https://doi.org/10.1016/s1360-1385\(99\)01543-5](https://doi.org/10.1016/s1360-1385(99)01543-5).
- Nitzsche, R., O. Gunay-Esiyok, M. Tischer, V. Zagoriy, and N. Gupta. 2017. A plant/fungal-type phosphoenolpyruvate carboxykinase located in the parasite mitochondrion ensures glucose-independent survival of *Toxoplasma gondii*. *The Journal of Biological Chemistry* 292 (37): 15225–15239. <https://doi.org/10.1074/jbc.M117.802702>.
- Ohmori, T., K. Adachi, Y. Fukuda, S. Tamahara, N. Matsuki, and K. Ono. 2004. Glucose uptake activity in murine red blood cells infected with *Babesia microti* and *Babesia rodhaini*. *The Journal of Veterinary Medical Science* 66 (8): 945–949. <https://doi.org/10.1292/jvms.66.945>.
- Romano, A.H., and T. Conway. 1996. Evolution of carbohydrate metabolic pathways. *Research in Microbiology* 147 (6–7): 448–455. [https://doi.org/10.1016/0923-2508\(96\)83998-2](https://doi.org/10.1016/0923-2508(96)83998-2).
- Singh, P., S. Lonardi, Q. Liang, P. Vydyam, E. Khabirova, T. Fang, S. Gihaz, J. Thek-kiniath, M. Munshi, S. Abel, et al. 2023. *Babesia duncani* multiomics identifies virulence factors and drug targets. *Nature Microbiology* 8 (5): 845–859. <https://doi.org/10.1038/s41564-023-01360-8>.
- Storm, J., S. Sethia, G.J. Blackburn, A. Chokkathukalam, D.G. Watson, R. Breitling, G.H. Coombs, and S. Müller. 2014. Phosphoenolpyruvate carboxylase identified as a key enzyme in erythrocytic *Plasmodium falciparum* carbon metabolism. *PLoS Pathogens* 10 (1): e1003876. <https://doi.org/10.1371/journal.ppat.1003876>.
- Wickramasekara Rajapakshage, B.K., M. Yamasaki, S.J. Hwang, N. Sasaki, M. Murakami, Y. Tamura, S.Y. Lim, K. Nakamura, H. Ohta, and M. Takiguchi. 2012. Involvement of mitochondrial genes of *Babesia gibsoni* in resistance to diminazene aceturate. *The Journal of Veterinary Medical Science* 74 (9): 1139–1148. <https://doi.org/10.1292/jvms.12-0056>.
- Yu, L., Q. Liu, W. Luo, J. Zhao, H.F. Alzan, and L. He. 2021. The structural basis of *Babesia orientalis* lactate dehydrogenase. *Frontiers in Cellular and Infection Microbiology* 11: 790101. <https://doi.org/10.3389/fcimb.2021.790101>.

Publisher's Note

Springer Nature remains neutral with regard to jurisdictional claims in published maps and institutional affiliations.